# Development of Female and Male Thermoregulatory Models (FETM) using COMSOL

Stefan Gutierrez[1,2], Juliette Jacques[1,2], Timothy Rioux[1], John Castellani[1], Xiaojiang Xu[1]

[1]US Army Research Institute of Environmental Medicine, Natick, MA, US

[2]Oak Ridge Institute for Science and Education (ORISE), Oak Ridge, TN, USA

## Abstract

Most current thermoregulation models represent the body in significantly simplified forms, e.g., cylinders or spheres. These simple geometries do not fully represent the complexity of bones, organs, etc. contained in the human body. Modern medical technologies allow for more advanced and accurate scans of human cadavers. These medical techniques enable anatomically correct mesh applications to be used for heat transfer simulations that include organs, tissues, and complicated geometry. Recently, finite element models of female and male thermoregulation with geometry based on medical images were successfully developed by Castellani et al. (Castellani et al., 2021; Castellani et al., 2023). This paper presents these two models and demonstrates temperature distributions simulated by these two models.

A female and male mesh were created from Duke University's XCAT phantom dataset. The two meshes were imported into COMSOL Multiphysics software for model development of a male and female body with human thermoregulatory mechanisms and heat transfer properties of 13 major organs and tissues, such as the as skin, bones, muscles, fat, and internal organs. Heat transfer simulations were conducted using COMSOL Multiphysics bio - heat transfer module. The models included thermoregulatory mechanisms such as sweat, vasodilation and shivering, and physiological properties such as density, conductivity, specific heat, blood perfusion, and metabolic rate of all organs, bones, muscles, and fat.

The simulation predicts the temperature distributions throughout the human body for male and female thermoregulation systems. Two studies were conducted in this paper. One study simulated an individual in constant ambient neutral conditions (29 °C) for 90 minutes and the other study simulated varying ambient temperature conditions from 10 °C to 50 °C for 90 minutes. Figure 4 shows the internal and skin temperature distribution at an ambient temperature of 10 °C throughout a time period of 0 minutes to 20 minutes. The model displays the temperature distribution of the internal organs which in turn can be analyzed as core temperatures at different locations, e.g., esophagus and rectal temperatures.

With the use of an anatomically accurate mesh and geometry, the two models can simulate human temperature profiles at various climate conditions, e.g., heat and cold environments. The model's simulation tool can be used to analyze and predict how a human body will react to different ambient temperatures and allow for better understanding on how to prevent heat and cold strain and improve human performance.

## Introduction

Under certain environmental conditions, the human body is able to maintain its heat balance maintaining stable skin and core temperatures. The body uses various heat transfer and physiological properties such as sweating, shivering, vasodilation, vasoconstriction, heat redistribution through convective heat transfer via blood flow, etc., in order to maintain this balance. Models are used to analyze and predict thermoregulation properties and temperature in order to better understand human physiology. These models have been used to research hypothermia and hypotension, construct cooling and heating systems, engineer thermal wear, etc. Throughout the years, thermal regulation models have evolved to provide more detail and become more accurate, from the initial work on body temperature by Burton (Burton 1934) to the more physiological realistic modelling simulation of human responses to heat and cold. (Castellani et al., 2021; Unnikrishnan et al., 2021; Werner and Buse 1988; Silva et al., 2018; Kang et al., 2019). Earlier work on thermoregulation relied on simplified shapes such as cylinders and spheres in order to model human physiology however this approach is not the most accurate. These simplified shapes don't allow for the most accurate thermoregulation properties due to the complexity of the human body's physical and internal properties. Heat transfer and thermoregulation in the human body are highly dependent on the specific geometry of the subject which makes it crucial to have the most accurate representation to allow for better human temperature regulation data. Currently there are a small number of models that are 3D, while most are represented in one dimension (1D models). Because of advances in medical imaging, 3D models have been developed with more anatomically and geometrically accurate properties. The 3D modelling in this paper is a continuation and overview of the 3D modelling done by Castellani and colleagues (Castellani et al., 2021; Castellani et al., 2023). Figure 1 shows the first predicted thermoregulatory model in cold, comfortable, and hot ambient conditions developed by Castellani et al.

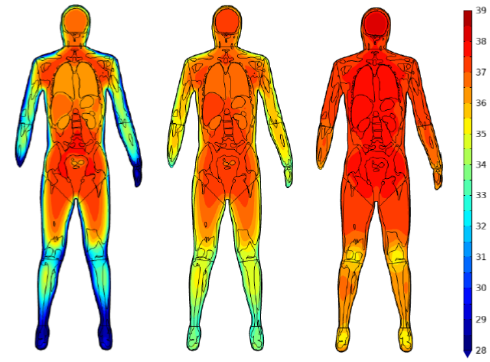


Figure 1. First predicted 3D model in cold (left), Comfortable (middle), and hot (right) environments.

This model uses human meshes derived from medical images of 13 organs and tissues to allow for better thermoregulation properties and results. Men and women have different physiological responses to temperature fluctuations understanding this thermoregulation process between sexes has been an on-going research goal for years. Most studies and data are taken using sex-neutral models due to the complexity in geometry. However, with accurate medical images COMSOL Multiphysics simulation can be being used to analyze and compare the differences in sex thermoregulation.

## Theory and Methods

To create a simpler analysis and model, the simulation was broken up into two groups, the passive system and the active system for human thermal regulation. The passive system of the model is responsible for the geometry, anatomy, and heat transfer properties. The active system is responsible for all the thermoregulation properties such as sweating, vasoconstriction, vasodilation, shivering, etc. The active system regulates these properties such as sweating, shivering, and skin blood flow using a hypothalamus and skin control signal process. In addition, muscle blood flow is regulated and controlled during exercise and shivering. These systems both exist in the male and female models. Both models were set to neutral and non – neutral temperature conditions for the thermoregulation simulations. XCAT Phantom images from Duke University were used for the geometric conditions of the human model. These Phantoms were developed for medical research and are amongst a population of phantoms that are representative of a variety of anatomical human physiology and conditions. These phantoms and images are designed to be realistic and match the physiology of live human subjects. The male model represents the size of the 50th percentile for the adult male population in the United States (37 years of age with a height of 1.76 m and weigh approximately 81 kg). Similarly, the female model represents the 50th percentile for adult female population (36 years of age with a height of 1.62m and weigh 66 kg). These Phantom medical data scans were processed and inverted into finite element meshes and segmented. The mesh process included voxelization, segmentation, region separation, and mesh generation. Simpleware SanIP Software (SYSNOPSYS) was used to segment the processed data into a working CAD model for the COMSOL simulation. The data was segmented to present various realistic regions such as the organs, bones, and muscles. In order to ensure there were no additional gaps within the segmentation, further processing was done. In order for volume element generation to be accurate and allow for easier simulation use, overall regions were created and divided. These regions include head, torso, left and right upper arms, left and right forearms, left and right hands, left and right upper legs, left and right lower legs, and left and right feet. The mesh went through independent test for validation in order to be optimized for COMSOL Multiphysics and resulted in the body containing 6.2 trillion tetrahedral elements. Figure 2 illustrates the mesh model of the male heart and organs.

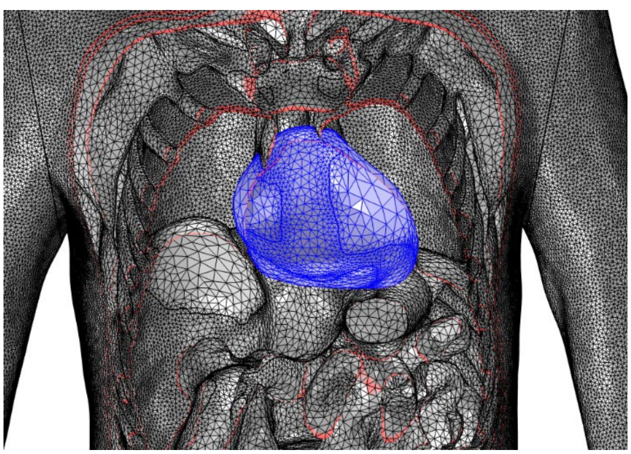

Figure 2. Male Mesh of Heart and Internal Organs

**Passive System**

The passive system dictates the anatomic structure of the body and the associated heat transfer properties of the body. Within the human body, heat balance is defined by the bio-heat equation. Within COMSOL this equation is:

$$\rho C_p \frac{\partial T}{\partial t} = \lambda \nabla^2 T + Q + \beta \omega \rho_b C_{p,b} (T_b - T) \tag{1}$$

Where $\rho$ is the density ($\mathrm{kg} * \mathrm{m}^{-3}$), $C_p$ is the specific heat ($J * kg^{-1} * {}^\circ\mathrm{C}^{-1}$), T is the temperature (°C), t is time (s), λ is the thermal conductivity ($W * m^{-1} * {}^\circ\mathrm{C}^{-1}$), ∇ is the temperature gradient, Q is the metabolic rate ($W * m^{-3}$). $\beta$ is the factor by which countercurrent heat exchange between arterial blood and venous blood is approximately considered, $\omega$ is the blood flow rate ($m^3 * s^{-1} * m^{-3}$), $\rho_b$ is the blood density ($kg * m^{-3}$), $C_{p,b}$ is the specific heat of blood ( ($J * kg^{-1} * {}^\circ\mathrm{C}^{-1}$), $T_b$ is the blood temperature (°C). Equation (1) is also defined as:

$$\begin{aligned} &\mathit{Rate\ of\ Change\ of\ Tissue\ Heat\ Storage} \\ &= \mathit{Heat\ Conduction} \\ &+ \mathit{Metabolic\ Heat\ Production} \\ &+ \mathit{Heat\ Exchange\ Between\ Blood\ and\ Tissue} \end{aligned}$$

The surface of the skin is the boundary of the simulation model. Evaporation, convection, and radiation aid in the heat exchange process at the boundary. The boundary condition contributed from the skin surface is described as:

$$\lambda \frac{\partial T}{\partial n} = (h_c + h_r) * (T_s - T_o) + E \tag{2}$$

where n is the normal to the boundary, $h_c$ is the convection coefficient conductivity ($W * m^{-2} * {}^\circ\mathrm{C}^{-1}$), $h_r$ is defined as the radiation coefficient ($W * m^{-2} * {}^\circ\mathrm{C}^{-1}$), $T_s$ is the surface temperature (°C), $T_o$ is the operative temperature (°C), and E is the heat loss due to the sweat evaporation ($W * m^{-2}$).

$T_o$ is represented by the following expression:

$$T_o = \frac{T_a * h_c + T_r * h_r}{h_c + h_r}$$

Where $T_a$ is the ambient temperature (°C), and $T_r$ is the radiative temperature from the environment (°C). When running simulations to replicate an indoor environment, $T_a = T_r$.

The convective coefficient can be represented by:

$$h_c = h_{c0} v^m$$

Where $h_c$ is the convective coefficient, $h_{c0}$ is a constant, $v^m$ is the wind velocity ($m * s^{-1}$) with m as a constant. $h_{c0}$ varies with the location of measurement. $h_r$ is derived by using the Stefan-Boltzmann law and is calculated using the following equation:

$h_r = f \cdot \varepsilon \cdot \sigma \cdot [(T_s + 273.2)^2 + (T_r + 273.2)^2] \cdot (T_s + T_r + 546.3)$

where $f$ is the view factor, $\varepsilon$ is emissivity, and $\sigma$ is the Stefan–Boltzmann constant ($5.67 * 10^{-8} W m^{-2} * K^{-4}$).

The equation used to model blood temperature is described as:

$$V_b \frac{dT_b}{dt} = \int \beta\omega(T - T_b)\, dV$$

Where $V_b$ is the volume of blood ($m^3$) in the body and is assumed to be 5L (.005 $m^3$). The simulation model assumes that the body has a central blood pool and that this blood is independent of the location and that the blood in the capillaries and veins is equal to the temperature of the tissues near the blood.

The model assumes that 100% of the respiratory heat exchange process occurs in the lungs. Evaporative and convective heat transfer occurs when the respiratory track exchanges air with the surrounding air in the environment. These parameters are proportional to the respiratory volume and increase when the body's metabolism increases. The respiratory heat loss is described as:

$$R_{resp} = 0.0014 Q_{tot}(34.0 - T_a)$$
$$+ 0.0173 Q_{tot}(5.87 - 10^{-3} P_a)$$

Where $R_{resp}$ is the respiratory heat loss (W), $Q_{tot}$ is the total metabolic heat production (W) produced by the body. $T_a$ is the ambient temperature of the environment (°C), $P_a$ is the ambient vapor pressure (Pa). the total metabolic rate is calculated using the following expression:

$$Q_{tot} = \int Q_0 dV + Q_{SH_{tot}} + Q_{EX_{tot}}$$

Where $Q_{SH_{tot}}$ is the total shivering heat production (W). Shivering is a thermoregulation process that occurs when the body's temperature is lowered. $Q_{EX_{tot}}$is the increases metabolic heat production due to exercise (W).

**Clothing**

In addition to physiological thermoregulation properties, the simulation also included clothing worn. Clothing acts as insulation between the environment and the skin which decreases heat exchange between the environment and the skin. When taking clothing into account the boundary equation becomes:

$$\lambda \frac{\partial T}{\partial n} = \frac{T_s - T_0}{R_{cl} + \frac{1}{f_{cl} * (h_c + h_r)}} + E$$

where $R_{cl}$ is the intrinsic clothing thermal resistance ($m^2 * °C * W^{-1}$), and $f_{cl}$ is a dimensionless clothing are factor expressed as the ratio of the clothing surface to the surface body area. In addition to insulation, clothing effects the evaporative heat loss process of the body.

**Active system**

The active system controls the thermoregulatory system that regulates the body's temperature. This system is broken into three parts: sensor, integrator, and effector. The skin has both cold and warm sensors dedicated to the detection of the cold and warmth of the body. These warm and cold skin thermoreceptors send signals to the hypothalamus through the sympathetic nervous system. The integrator system takes in and combines all the thermoreceptors and outputs the effector commands. The effector systems carry out the appropriate commands such as vasoconstriction, vasodilation, sweating, and shivering. The error signals associated with these commands are as such:

$$e_{hy} = T_{hy} - T_{hy,set}$$
$$e_s = T_{ms} - T_{ms,set}$$

Where $e_{hy}$ is the error signal from the sensor in the hypothallus (°C). $T_{hy}$ is the temperature in the hypothalamic region of the brain (°C). $T_{hy,set}$ is the reference temperature of the hypothalamus (°C). $e_s$ is the error from all sensors of the skin (°C). $T_{ms}$ is the mean skin temperature (°C). $T_{ms,set}$ is the reference temperature for the mean skin temperature (°C).

The skin blood flow has a direct correlation with vasodilation and vasoconstriction. They are calculated by the following equations:

$$DI = 113696 \cdot e_{hy} + 19480 \cdot e_s$$

$$CS = 1.1 \cdot (-e_{hy}) + 3.3 \cdot (-e_s)$$

$$\omega_s = \frac{\omega_{s_0} + \alpha_{DI} \cdot DI}{1 + CS}$$

Where DI is the total efferent skin vasodilation signal ($m^3 \cdot s^{-1} \cdot m^{-3}$), CS is the total efferent skin vasoconstriction signal which is dimensionless. $\omega_s$ is defined as the skin blood flow rate ($m^3 \cdot s^{-1} \cdot m^{-3}$), $\omega_{s_0}$ is defined as the skin blood flow rate ($m^3 \cdot s^{-1} \cdot m^{-3}$), and $\alpha_{DI}$ is the distribution factor of vasodilation. The values of vasodilation and vasoconstriction are defined as positive values because it is impossible for them to be negative in the human body.

When the body is experiencing cold temperatures, heat production is activated. Heat productions is activated using the body's shivering mechanism which is defined as:

$$Q_{SH_{tot}} = \frac{147.7 \cdot (-e_{hy}) + 44.6 \cdot (-e_s) - 1.48 \cdot (e_s)^2}{\sqrt{PBF}} * BSA$$

Where $Q_{SH_{tot}}$ is the metabolic heat from shivering (W). PBF is the body fat percentage, BSA is the body surface area ($m^2$). Any negative values within the analysis convert into zero. $Q_{SH_{tot}}$ is broken up by region and this is derived by:

$$Q_{SH} = \frac{\alpha_{SH} \cdot Q_{SH_{tot}}}{V_i}$$

where $\alpha_{SH}$ is the distribution factor of the shivering heat production and $V_i$ is the segment of the muscle ($m^3$). $Q_{EX_{tot}}$ is measured and estimated from the mechanical output and mechanical efficiency. When the heat production is increased due to exercise, it can be calculated using the following equation:

$$Q_{EX} = \frac{\alpha_{SH} \cdot Q_{EX_{tot}}}{V_i}$$

When the body has greater muscle contractions and the metabolic workload of the body is increased, more oxygen is needed, as a result, more blood flow is needed. Blood flow is expressed as:

$$\omega_m = \omega_{m0} + c_m \cdot (Q_{SH} + Q_{EX})$$

Where $\omega_{m0}$ is the basal blood flow rate of muscle ($m^3 \cdot s^{-1} \cdot m^{-3}$), and $c_m$ is the proportionality coefficient ($m^3 \cdot s^{-1} \cdot m^{-3} W^{-1}$). The proportionality coefficient was assumed to be 1.39 $m^3 s^{-1} \cdot W^{-1}$.

Due to evaporative heat loss, the body loses heat from the environment. This heat loss can be calculated by:

$$E = E_{dif} + E_{rsw}$$

Where $E_{dif}$ is the basal evaporation ($W \cdot m^{-2}$), and $E_{rsw}$ is the evaporation of sweat regulated by the thermoregulatory system ($W \cdot m^{-2}$). $E_{dif}$ is the evaporative heat loss as a result of water diffusing to the environment from the skin.

3D modeling makes it possible to predict the temperature distribution, i.e., local temperatures at Figure 3, 7 and 8. "Probes" are feature of COMSOL. In addition to various probes, the simulation takes measurements of specified regions such skin, blood, bones, and organs. The model was set to environmental parameters that consists of Ambient temperature, thermal neutral radiative temperature, relative humidity, initial air velocity, ambient temperature for dynamic studies, Lewis's ratio, and latent heat of water. These values were set to 29 °C, 29 °C, .4,.18,43 °C, 16.5 $\frac{K}{kPa}$ and 64 $\frac{J}{g}$, respectively.

### Experimental Studies

Two studies were conducted for the simulation experiment. The first study was conducted at thermal neutral ambient conditions simulating a person in an environment for an extended period of time with no clothing. The study simulated an individual idle in an environment set at 29 °C for 90 minutes. The study took 1 min intervals throughout the process. This will show insight on the body's heat balance process at neutral conditions. In addition, another time study was conducted simulating an idle individual with varying ambient temperatures instead of constant neutral conditions to analyze how the body temperature changes as temperature went from low to high. The temperature varies from 10°C to 50 °C. All other environmental parameters stated in previous sections were set to constant values for both studies.

## Simulation Results

For the first study, set in thermal neutral conditions (29 °C), temperatures during a simulated 90-minute exposure did not fluctuate significantly for both males and females. This result was expected due to the concept of thermal neutrality. This condition states that the human body's heat production is not increased or decreased via heat or cold stress. After the 90 minutes concluded, the skin temperature parameter resulted in the lowest temperature ranging from 33.77 ℃ to 33.8 ℃. Internal temperatures such as the rectal, blood, brain, and heart have ranges of 37.22 ℃ to 37.23 ℃, 36.92 ℃ to 36.93 ℃, 37.30 ℃ to 37.31 ℃, 36.8 ℃ to 36.9 ℃, respectively. This study shows a good baseline for the accuracy of the simulation parameters. In addition to blood, brain and heart temperatures, local regional temperatures via COMSOL probes were analyzed at thermal neutral conditions. Figure 3 shows that in both males and females, similar temperatures were seen in local regions at 29 ℃ after 90 min.

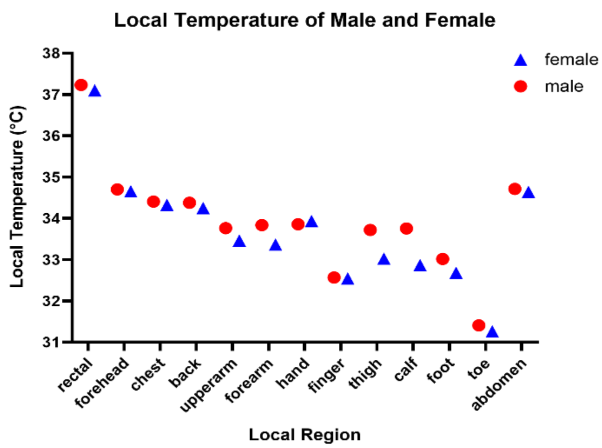


Figure 3. Time Study at 29°C ambient temperature

In study 2, ambient temperatures were varied. As the ambient temperature increase, all regional parameters for the female model reached a converging point approximately at 38 ℃ as shown in figure 4. This trend is showing that the simulation is replicating what the human body does when exposed to hot ambient temperatures over time. As the ambient environment increases in temperature, our body will adjust and increase skin temperatures as well as internal temperature. Male results show similar responses to an increase in ambient temperature (Figure 5). These results demonstrate the predicted temperatures for each body region after 90 minutes exposure for each respective ambient temperature.

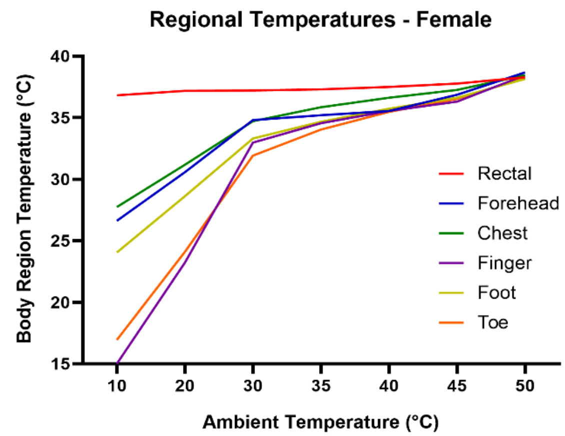


Figure 4. Temperature distribution at varies ambient temperatures (female)

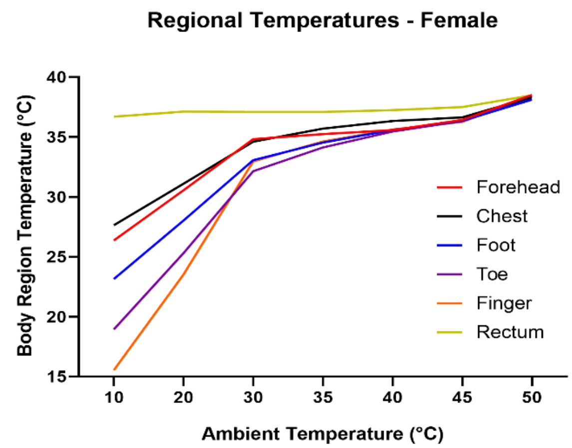


Figure 5. Temperature distribution at varies ambient temperatures (male)

Despite having different physical geometries, both male and female simulations show similar responses. Figure 5 also shows the temperature distribution in different body regions when the ambient temperature is 10 ℃. As expected, the model predicts that as time goes on, body temperatures decrease as shown in figure 6. At time 0 min, 5 min, and 20 min, the model's predicted core region resulted in the highest temperature reaching 37.6 ℃, 37.6 ℃, and 37.7 ℃, respectively. The lowest temperatures at the given times came from the toe region and were 30.9 ℃, 27 ℃, and 20.3 ℃, respectively. The model decreased in temperature significantly throughout the 90 mins with the low end of the toe region decreasing by 10.6 degrees Celsius showing that prolonged cold environment can dramatically decreases the body's peripheral region temperature such as toes.

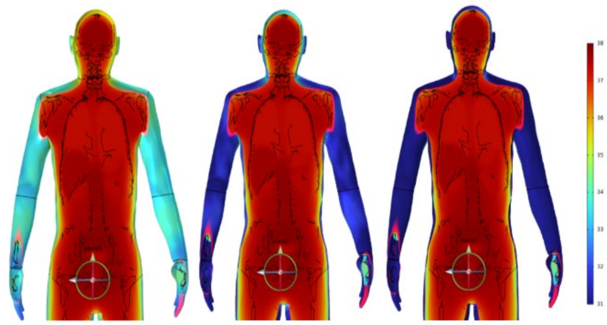

Figure 6. Temperature distribution at 10 °C at 0 minutes (left), 5 minutes (middle), and 20 minutes (right)

## Conclusion

This paper served as a short overview for a male and female 3D thermoregulatory model initially developed by Castellani et al. (Castellani et al., 2021; Castellani et al., 2023). This 3D model predicts temperature distributions across the body externally on the skin as well as internally for organs, blood, muscles and bones. The model considers the inhomogeneity of the human body for both male and female.

Even though the simulation shows a thermal regulatory process that is seen in real human models, the simulation requires future validation, specificity in extreme cold and hot temperatures. In addition, future investigation of physiological and thermal regulation differences for male and female physiology will be done.

## References


[1] Castellani MP, Rioux TP, Castellani JW, Potter AW, Notley SR, Xu X. Finite element model of female thermoregulation with geometry based on medical images. J Therm Biol. Apr 2023; 113:103477.

[2] Castellani MP, Rioux TP, Castellani JW, Potter AW, Xu X. A geometrically accurate 3-dimensional model of human thermoregulation for transient cold and hot environments. Comput Biol Med. Nov 2021; 138:104892.

[3] Werner J and Reents T. A contribution to the Topography of Temperature Regulation in Man, European Journal of Applied Physiology, pp. 87-94, 1980

[4] Xu X., Tikuisis P. Thermoregulatory modeling for cold stress. Compr. Physiol. 4 (3), 1057–1081, 2014.

[5] Xu X, Rioux TP, Castellani MP. Three dimensional models of human thermoregulation: A review, J. Therm. Biol., 2023.

[6] Unnikrishnan, G., Hatwar, R., Hornby, S., Laxminarayan, S., Gulati, T., Belval, L.N., Giersch, G.E.W., Kazman, J.B., Casa, D.J., Reifman, J., 2021. A 3-D virtual human thermoregulatory model to predict whole-body and organ-specific heat-stress responses. Eur. J. Appl. Physiol. 2021

[7] Werner, J., Buse, M. Temperature profiles with respect to inhomogeneity and geometry of the human body. J. Appl. Physiol. 65 (3), 1110–1118, 1988.

[8] Silva, A.B.C.G., Wrobel, L.C., Ribeiro, F.L.B. A thermoregulation model for whole body cooling hypothermia. J. Therm. Biol. 78, 122–130, 2018

[9] Kang, Z., Wang, F., Udayraj. An advanced three-dimensional thermoregulation model of the human body: development and validation. Int. Commun. Heat Mass Tran. 107, 34–43. 2019


## Acknowledgments


The authors would like to thank Drs. Chris Goddard, Ross Cotton, and Kerim Genc (Synopsys, CA) for developing the female and male mesh and their continued support. The authors would also like to thank Dr. Nagi Elabbasi and Dr. Andrew Spann (Veryst Engineering, MA) for their help in using the COMSOL software.


Approved for public release; distribution is unlimited. The opinions or assertions contained herein are the private views of the author(s) and are not to be construed as official or reflecting the views of the Army or the Department of Defense. Any citations of commercial organizations and trade names in this report do not constitute an official Department of the Army endorsement of approval of the products or services of these organizations.

## Disclaimer

Author views not official US-Army/DOD policy. Any citations of commercial organizations and trade names in this report do not constitute an official Department of the Army endorsement of approval of the products or services of these organizations.